Closed-Form Crosstalk Noise Metrics for Physical Design Applications

Lauren Hui Chen
Avant! Corporation
Fremont, CA 94538, USA
lauren@avanticorp.com

Malgorzata Marek-Sadowska
Electrical and Computer Engineering Department
University of California, Santa Barbara, CA 93106, USA
mms@ece.ucsb.edu

ABSTRACT

In this paper we present efficient closed-form formulas to estimate capacitive coupling-induced crosstalk noise for distributed RC coupling trees. The efficiency of our approach stems from the fact that only the five basic operations are used in the expressions: addition ($x+y$), subtraction ($x-y$), multiplication ($x\times y$), division (x/y) and square root ($\sqrt{x}$). The formulas do not require exponent computation or numerical iterations. We have developed closed-form expressions for the peak crosstalk noise amplitude, the peak noise occurring time and the width of the noise waveform. Our approximations are conservative and yet achieve acceptable accuracy. The formulas are simple enough to be used in the inner loops of performance optimization algorithms or as cost functions to guide routers. They capture the influence of coupling direction (near-end and far-end coupling) and coupling location (near-driver and near-receiver).

1. INTRODUCTION

Scaling the feature sizes and lowering the level of power supply voltage has made digital designs vulnerable to noise. Noise sources are spread widely over the chip, among which interconnect coupling noise (crosstalk) becomes a performance-limiting factor and plays an important role in the entire design flow affecting timing closure.

Different design stages have different requirements for accuracy of modeling crosstalk noise effects. Trade-offs exist between the accuracy and complexity. Analytical expressions are preferred because simulation is always expensive and ineffective for use with modern designs containing millions of transistors and wires. In the design sign-off stage, the most accurate noise metric is required. However, discovering the coupling-induced problems in the late stages of the design may create an unworkable situation because most of the layout has already been fixed, and there may not be much room left to make changes in placement and routing. Furthermore, every iteration of the design flow is very expensive. Therefore, fast and conservative coupling-induced crosstalk noise estimators with reasonable accuracy are desirable to address crosstalk in the earlier design stages and optimization flow such as logic restructuring [3].

The existing crosstalk noise estimation methods are either not simple enough to afford optimization considering crosstalk effects in the design flow, or not sufficiently accurate. The majority of research efforts have been focused on developing formulas for the peak noise pulse amplitude (V_p), while the peak noise occurring time and the pulse width have not been well-researched. The pulse-width (W_n) is a measure of energy, and the propagating noise occurring time (t_p) is essential in determining cumulative effects of crosstalk signals caused by different sources. The peak noise occurring time and noise energy have similar importance for circuit performance as the peak amplitude of the crosstalk noise has for functional failure.

In this paper we present simple closed-form formulas to estimate the essential parameters of the capacitive coupling-induced crosstalk noise waveform: the peak amplitude, the peak noise occurring time, and the noise waveform width. Our model can handle distributed coupled RC trees. In our expressions only the following five basic operations are used: addition ($x+y$), subtraction($x-y$), multiplication($x\times y$), division(x/y) and square root($\sqrt{x}$). The expressions do not require computation of exponents or numerical iterations. And they are explicit functions of the moments of the noise output waveform, which are obtained using existing methods [11][13][15]. This paper focuses on crosstalk noise estimation for distributed RC coupling trees, where the non-linear drivers are modeled by equivalent resistances [2].

2. OVERVIEW OF THE EXISTING CROSSTALK NOISE METRICS

We assume that the following are known: the structure of the coupling circuit, the device, the interconnect and the technology parameters, as well as the parameters for the input signals which include the arrival times and the transition times. The objective is to obtain the parameters of the output noise waveform.

2.1 The flow

Figure 1 presents analysis flows of the existing crosstalk estimation methods. In the presence of multiple aggressors, the principle of superposition can be applied.

We divide the entire flow into two stages: *FrontEnd* and *BackEnd*. The FrontEnd stage deals with the circuit structure and external excitations and quantifies the physical features into particular parameters of the S domain. $V_o^{(j)}$ represents the contribution of the *j*th aggressor to the output of the victim net. It is the victim's output voltage in the S domain when only the *j*th aggressor is switching and all the other aggressors are quiet. $H^{(j)}$ denotes the transfer function in the same conditions for the *j*th aggressor; *n* denotes the number of aggressors. The BackEnd flow extracts the physical features of the output waveform from what has been obtained in the FrontEnd Flow. Various methods exist for both stages of the flow.

2.1.1 The FrontEnd flow

This stage includes modeling of the coupling circuit and computation of the transfer functions based on the selected model.

A well-accepted method to deal with non-linear drivers and receivers is to model each of them with linear RC components, where the driver is replaced by an equivalent resistor, and the receiver by a loading capacitor. The coupled interconnect is modeled by distributed RC components. From now on we will consider only linearized coupled RC networks.

- Lumped v.s distributed model

In the lumped model, the total capacitance and resistance values are used, disregarding the actual coupling location and distribution. Most of crosstalk-noise-modeling papers published in the earlier years belong to this category [5][6][9][14]. With the advance of deep submicron technology, lumped models no longer satisfy the accuracy requirement. Distributed coupled RC tree structure models become necessary even for the early design stages. Many papers address this problem[1][7][10][13][17].

- Single-aggressor v.s. multiple-aggressor model

In real circuits, we rarely have victim nets which are coupled to single aggressors only. Typically there exist nets coupled with hundreds of aggressors, most of which contribute only a small crosstalk noise. To reduce computational complexity in the

presence of multiple aggressors, the principle of superposition is widely used. Usually, one aggressor is processed at a time, and the final output in Laplace domain is expressed as a summation of the individual outputs produced by switching one aggressor at a time. However, two different interpretations exist for the same principle.

Some existing papers [5][6][7][9][10][14] apply superposition with one aggressor at a time, assuming other coupled aggressors don't exist. In such a case, the transfer function of the coupling circuit can be greatly simplified, and it is easier to obtain a closed-form output waveform. Note that a closed-form output waveform does not guarantee a closed-form noise expression.

Such a decoupling of a multiple-aggressor problem into a sequence of single-aggressor problems can be primarily used to screen out some minuscule noise sources. However, the crosstalk noise computed using such an approach can serve neither as an upper bound nor as a lower bound for the actual noise in the original coupling circuit. This limits its applicability in noise estimation even in the routing stage, because conservatism is an essential requirement.

Therefore, the existence of multiple aggressors has to be explicitly accounted for and expressed in the transfer functions, even in the formulas used in the early stages of the design flow. This is the second interpretation of the superposition principle. Existing publications based on this scenario include [1][13][17].

- Moment computation

The purpose of moment computation is to determine the coefficients in the transfer function (or admittance function) expressed as follows:

$$H(s) = \frac{a_0 + a_1 s + \ldots + a_{q-1} s^{q-1}}{b_0 + b_1 s + \ldots + b_q s^q} = (h_0 + h_1 s + \ldots + h_{2q+1} s^{2q+1}) \quad (1)$$

where $h_p = (-1)^p (m_p / p!)$, $p = 0 \sim 2q+1$. $a_0^{(j)} = 0$, hence $A_0^{(j)} = 0$ for the transfer functions in figure 1 because there is no DC (direct current) path from any aggressor's input to the victim's receiver node.

Equation (1) is the qth order Pade Approximation of transient response in s domain [12]. Different methods for the model order reduction and moment computation have been extensively discussed in numerous papers; representative examples are [8][12][16]. Passivity is required for the reduced-order model to guarantee stability of the system. In order to guarantee the passivity, the moments are computed for the admittance matrix instead of for the transfer functions in the method proposed in [1]; then the output waveform at the victim receiver node is derived. Moment computation is usually expensive, even with a linear order recursive algorithm [17]. Therefore, [13] and [15] derived closed-

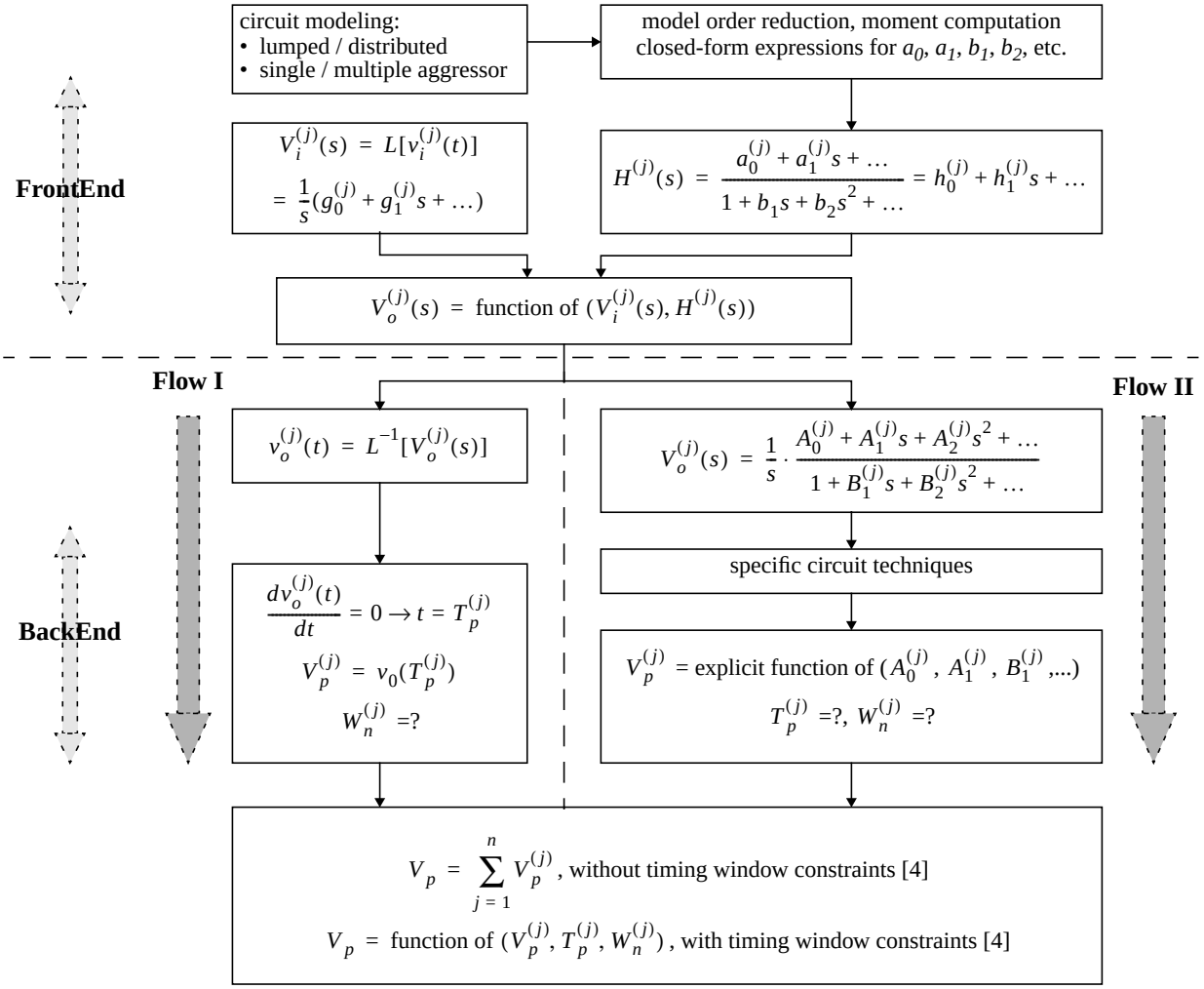

Figure 1. Existing flows for crosstalk noise analysis, with superposition applied in time domain

form expressions to directly compute the coefficients a_0 and a_1 for the numerator in equation (1), and the closed-form expressions for b_1 and b_2 can be found in [11].

In general, any approximation with more than two poles cannot produce closed-form expressions for delay and noise [1]. Therefore, second order Pade Approximation is preferred in fast crosstalk noise evaluations.

2.1.2 The BackEnd flow

The $V_o^{(j)}(s)$ and $V_{sum}(s)$ obtained in the FrondEnd flow contain all the circuit and external excitation information needed to extract the parameters of the output waveform. Many methods were proposed to solve this problem. The *flow I* in figure 1 summarizes methods which apply inverse Laplace transformation and determine the explicit closed-form expression for the output waveform in time domain [1][10][17]:

$$v_o^{(j)}(t) = L^{-1}[V_o^{(j)}(s)],\ v_o(t) = v_{sum}(t) = L^{-1}[V_{sum}(s)]$$

However, a closed-form expression for $v_o(t)$ / $v_o^{(j)}(t)$ does not guarantee closed-form expressions for all the crosstalk noise parameters. Additionally, computing W_n from these equations requires numerical iterations, and the result cannot be expressed by a closed-form expression.

The *flow II* type methods were proposed to conquer the shortcomings of the *flow I* methods. References [7] and [13] are two representative papers in this category. Both papers provide efficient closed-form expressions to compute the peak noise amplitude V_p for distributed coupled RC networks. Their efficiency meets our criteria. Reference [7] presents an absolute upper bound for V_p, however, with an unbounded maximum error percentage and no closed-form expression for t_p and W_n. Reference [13] derives elegant expressions for V_p and effective W_n with a bounded maximum percentage error.The formulas are as follows:

$$W_n^{(j)} = B_1^{(j)} - \frac{A_2^{(j)}}{A_1^{(j)}},\ V_p^{(j)} = \frac{A_1^{(j)}}{W_n^{(j)}} = \frac{A_1^{(j)}}{B_1^{(j)} - A_2^{(j)}/A_1^{(j)}}$$

The notation is explained in figure 1. However, the peak noise occurring time t_p cannot be easily obtained using this approach. Furthermore, $A_2^{(j)}$ depends on $a_2^{(j)}$ (figure 1). Due to the difficulty in obtaining a closed-form expression for $a_2^{(j)}$, the crosstalk noise expressions are approximated by $W_n^{(j)} \approx B_1^{(j)}$ and $V_p^{(j)} \approx A_1^{(j)}/W_n^{(j)} = A_1^{(j)}/B_1^{(j)}$ for computation efficiency, at the cost of reduced accuracy.

Shortcomings of the existing methods motivate our research in developing new crosstalk noise estimates. Our goal is to develop simple formulas which would be applicable in the physical design stage of optimization flows.

We would like to handle arbitrary coupling tree structures modeled by distributed RC components. We will admit multiple aggressors and distinguish between the coupling directions. Also we will differentiate the near driver from the near receiver coupling location.

We compute the moments of the output noise waveform based on closed-form expressions given by [11][13][15], and our formulas will be explicit functions of the obtained moments. We are seeking tight upper bounds for peak amplitude, peak noise occurring time, pulse width, and energy.

3. THE NEW CROSSTALK NOISE METRIC

In this section, we analyze the crosstalk noise computation, and present a practical approximation of the output waveform which carries the minimum necessary information. This simplification provides the basis for our new approach to achieve closed-form expressions for peak amplitude V_p, peak noise occurring time t_p and pulse width W_n.

3.1 A practical view of the output waveform

For crosstalk noise, the data sought are the following parameters of the waveform: T_0, T_1, T_2, V_p, where T_0 is the crosstalk signal arrival time, T_1 and T_2 are the two transition times, and V_p is the peak amplitude. The peak noise occurring time t_p and the pulse width W_n can be computed from T_0, T_1, T_2, V_p, as indicated in figure 2. Superscript *(j)* has been omitted for simplicity.

We propose two methods to simplify the noise waveform. The first one applies a piecewise-linear approximation as illustrated in figure 2 (b). The second one uses a mixed linear and exponential approximation depicted in figure 2 (c).

In the first method, both the rising and falling transitions are approximated by straight lines.

In the second method, the left transition is approximated by a straight line, and the right transition is approximated by an exponential waveform with time constant τ_2. The noise waveform depicted in figure 2 (c) is given by

$$v_o(t) = \begin{cases} V_p \cdot (t - T_0)/T_1 & (T_0 \le t < T_0 + T_1) \\ V_p \cdot e^{-(t - T_0 - T_1)/\tau_2} & (t \ge T_0 + T_1) \\ 0 & (t < T_0) \end{cases} \quad (2)$$

We use T_2 to represent the equivalent transition time for the exponential waveform. We have

$$T_2 = \lambda \cdot \tau_2 \quad (3)$$

The value of λ depends on the definition of transition time. Suppose the transition time is measured as a time needed for the noise voltage to reach 90% of V_p starting from the moment it had reached 10% of V_p. We denote the corresponding times as $T_{0.9}$ and $T_{0.1}$, respectively.

$$v_o = 0.9V_p \rightarrow T_{0.9} = T_0 + T_1 + \ln\left(\frac{1}{0.9}\right) \cdot \tau_2 \quad (4)$$

$$v_o = 0.1V_p \rightarrow T_{0.1} = T_0 + T_1 + \ln\left(\frac{1}{0.1}\right) \cdot \tau_2 \quad (5)$$

So the transition time is given by:

$$T_2 = \frac{T_{0.1} - T_{0.9}}{0.8} = 1.25\left(\ln\frac{1}{0.1} - \ln\frac{1}{0.9}\right) \cdot \tau_2 \quad (6)$$

And we define the default value for λ as:

$$\lambda = 1.25\left(\ln\frac{1}{0.1} - \ln\frac{1}{0.9}\right) \approx 2.7465 \quad (7)$$

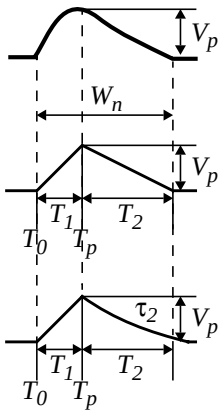

(a) The crosstalk noise waveform

(b) Piece-wise-linear approximation
min. information (T_0, T_1, T_2, V_p)
$T_p = T_0 + T_1,\ W_n = T_1 + T_2$

(c) Mixed linear and exponential approximation
min. information (T_0, T_1, τ_2, V_p)
$T_2 = \lambda \cdot \tau_2$

Figure 2. The information carried by a noise waveform

According to equations (3) and (7), the time constant τ_2 can be equivalently represented by the transition time T_2.

3.2 Our model

Based on the minimum information carried by the output signal, we can derive directly the expressions for the desired parameters of crosstalk noise. We do not perform the inverse Laplace transforms. Instead, we compare the appropriate coefficients in Laplace domain. Figure 3 illustrates the flow of our method.

The initial few steps of our approach are the same as in the FrontEnd flow described in figure 1. After obtaining $V_o^{(j)}(s)$ in the Laplace domain, we store the corresponding coefficients $f_k^{(j)}$s. Then we assume that the output waveform is approximated by two linear segments, as shown in figure 2(b). We transfer this approximate waveform into the Laplace domain and obtain the corresponding $V_o^{(j)'}(s)$, whose coefficients $e_k^{(j)}$s are functions of $T_0^{(j)}$, $T_1^{(j)}$, $T_2^{(j)}$, and $V_p^{(j)}$. Now we make the corresponding coefficients of $V_o^{(j)}(s)$ equal to those of $V_o^{(j)'}(s)$ and we derive equations depending only on the variables $T_0^{(j)}$, $T_1^{(j)}$, $T_2^{(j)}$, and $V_p^{(j)}$. The solution of these equations will give us closed-form expressions for the desired parameters. We will derive our formulas based on the second order Pade approximation. According to figure 3,

$$V_o^{(j)}(s) = V_i^{(j)}(s) \cdot H^{(j)}(s) = \frac{1}{s} \cdot \sum_{k=0}^{3} (f_k^{(j)} \cdot s^k) \qquad (8)$$

where superscript $j>0$ denotes the parameters related to the jth aggressor. $V_i^{(j)}(s)$ is the jth input signal. $H^{(j)}(s)$ is the transfer function from the jth input to the victim's output when the other inputs are quiet.

We use the lower case $t_0^{(j)}$ and $t_r^{(j)}$ to represent the arrival time and the transition time for the input signals, the upper case $T_0^{(j)}$, $T_1^{(j)}$, $T_2^{(j)}$, and $V_p^{(j)}$ represent the parameters of the victim's output noise waveform $V_o^{(j)}(s)$ produced by the switching of the jth aggressor.

3.2.1 The transfer function

We obtain the transfer function following approaches described in the existing papers. For the reasons already mentioned, we chose the second order Pade Approximation to obtain our transfer function:

$$H^{(j)}(s) = \frac{a_0^{(j)} + a_1^{(j)} s}{1 + b_1 s + b_2 s^2} = h_0^{(j)} + h_1^{(j)} s + h_1^{(j)} s^2 + h_3^{(j)} s^3$$

where [12]

$$h_0^{(j)} = a_0^{(j)} = 0$$

$$h_1^{(j)} = a_1^{(j)} - h_0^{(j)} b_1 = a_1^{(j)}$$

$$h_2^{(j)} = -(h_0^{(j)} b_2 + h_1^{(j)} b_1) = -a_1^{(j)} b_1$$

$$h_3^{(j)} = -(h_1^{(j)} b_2 + h_2^{(j)} b_1) = a_1^{(j)} (b_1^2 - b_2)$$

All the transfer functions of the same coupling circuit share the same coefficients for the denominator. b_1 is found from the summation over all the unique open-circuit time constants, and b_2 is the sum of all the unique products of the open-circuit and short-circuit time constants. The coefficients for the denominator are taken from [11]. The coefficients for the numerator of the transfer function from the jth aggressor's input to the victim's output are given by [13].

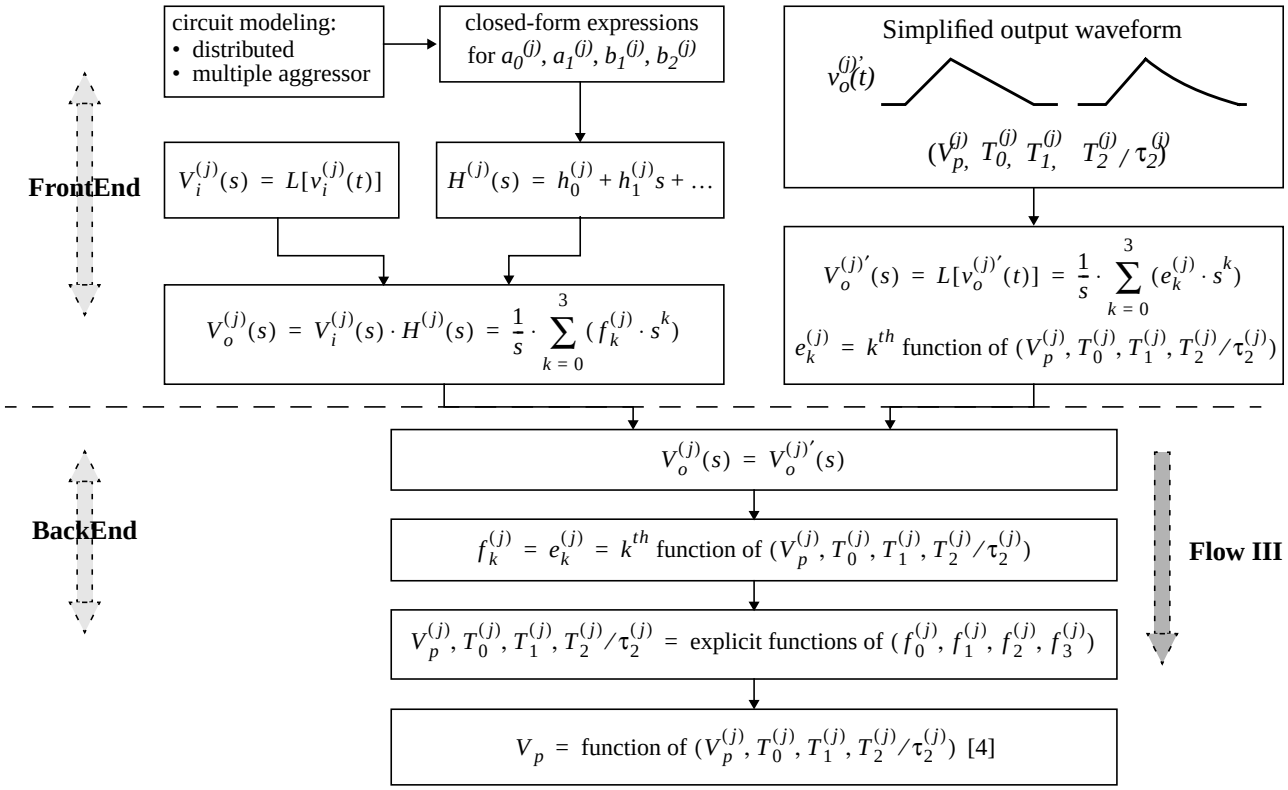

Figure 3. Our flow for crosstalk noise computation

3.2.2 The input

We consider arbitrary types of input, such as a rising ramp, a falling ramp, rising exponential waveform, falling exponential waveform, etc. We use $t_0^{(j)}$ and $t_r^{(j)}$ to represent the arrival time and the transition time for the *j*th input $V_i^{(j)}$, respectively. The input in Laplace domain is given by

$$V_i^{(j)}(s) = \frac{1}{s}(g_0^{(j)} + g_1^{(j)}s + g_2^{(j)}s^2 + g_3^{(j)}s^3) \quad (9)$$

$V_i^{(j)}(s)$ is normalized with respect to power supply voltage V_{dd}.

3.2.3 The output $V_o^{(j)}(s)$

From equation (8), we have

$$V_o^{(j)}(s) = V_i^{(j)}(s) \cdot H^{(j)}(s) = \frac{1}{s}(f_0^{(j)} + f_1^{(j)}s + f_2^{(j)}s^2 + f_3^{(j)}s^3) \quad (10)$$

where the moments of the output waveform are given by:

$$f_0^{(j)} = 0 \quad (11)$$

$$f_1^{(j)} = h_1^{(j)} \cdot g_0^{(j)} \quad (12)$$

$$f_2^{(j)} = h_1^{(j)} \cdot g_1^{(j)} + h_2^{(j)} \cdot g_0^{(j)} \quad (13)$$

$$f_3^{(j)} = h_1^{(j)} \cdot g_2^{(j)} + h_2^{(j)} \cdot g_1^{(j)} + h_3^{(j)} \cdot g_0^{(j)} \quad (14)$$

For example, assume the *j*th aggressor's arrival time is 0 ($t_0^{(j)} = 0$), when the victim net is at ground level, and the *j*th aggressor net has a rising ramp transition, the moments of the output waveform are given by:

$$f_0^{(j)} = 0 \quad (15)$$

$$f_1^{(j)} = a_1^{(j)} \quad (16)$$

$$f_2^{(j)} = -a_1^{(j)}\left(b_1 + \frac{t_r^{(j)}}{2}\right) \quad (17)$$

$$f_3^{(j)} = a_1^{(j)}\left(b_1^2 - b_2 + \frac{b_1 t_r^{(j)}}{2} + \frac{(t_r^{(j)})^2}{6}\right) \quad (18)$$

3.2.4 The piece-wise-linear approximation $V_o^{(j)'}(s)$

The Laplace transform of the simplified output waveform is given by

$$V_o^{(j)'}(s) = L[v_o^{(j)'}(t)] = \frac{1}{s} \cdot \sum_{k=0}^{3} (e_k^{(j)} \cdot s^k) \quad (19)$$

Suppose that the victim net is at ground level, and the *j*th aggressor net is transiting from low to high. The corresponding coefficients (moments of the approximated output waveform) are (superscript *(j)* is omitted in equations (20)-(54) to simplify the expressions):

$$e_0 = 0 \quad (20)$$

$$e_1 = \frac{(m+1)}{2} \cdot V_p \cdot T_1 \quad (21)$$

$$e_2 = -\frac{(m+1)}{6} \cdot V_p \cdot T_1 \cdot [(m+2)T_1 + 3T_0] \quad (22)$$

$$e_3 = \frac{(m+1)}{24} V_p T_1 [(m^2+3m+3)T_1^2 + 4(m+2)T_0 T_1 + 6T_0^2] \quad (23)$$

where *m* is defined by:

$$T_2 = mT_1 \qquad (0 < m < \infty) \quad (24)$$

3.2.5 The mixed linear and exponential approximation $V_o^{(j)'}(s)$

The Laplace transform of the approximated output waveform is given by

$$V_o^{(j)'}(s) = L[v_o^{(j)'}(t)] = \frac{1}{s} \cdot \sum_{k=0}^{3} (e_k^{(j)} \cdot s^k)$$

where the moments of this output waveform are given by:

So the coefficients can be simplified as follows:

$$e_0 = 0 \quad (25)$$

$$e_1 = V_p T_1\left(\frac{m}{\lambda} + \frac{1}{2}\right) \quad (26)$$

$$e_2 = -(V_p T_1)\left[\left(\frac{m^2}{\lambda^2} + \frac{m}{\lambda} + \frac{1}{3}\right)T_1 + \left(\frac{m}{\lambda} + \frac{1}{2}\right)T_0\right] \quad (27)$$

$$e_3 = V_p T_1\left[\left(\frac{m^3}{\lambda^3} + \frac{m^2}{\lambda^2} + \frac{m}{2\lambda} + \frac{1}{8}\right)T_1^2\right] + V_p T_1\left[\left(\frac{m^2}{\lambda^2} + \frac{m}{\lambda} + \frac{1}{3}\right)T_1 T_0 + \frac{1}{2}\left(\frac{m}{\lambda} + \frac{1}{2}\right)T_0^2\right] \quad (28)$$

where *m* is defined in equation (24). Note that we have replaced τ_2 with T_2 / λ (mT_1 / λ) according to equation (3) in order to compare with the piecewise-linear model.

3.3 New noise metric I

Based on the piece-wise-linear approximation, let $V_o^{(j)}(s) = V_o^{(j)'}(s)$, and match the corresponding coefficients, we have:

$$e_k^{(j)} = f_k^{(j)} \qquad (k = 1, 2, 3) \quad (29)$$

where $f_k^{(j)}$s are the moments of the noise output waveform, which can be computed by equations (11) to (14), and are simplified to equations (15) to (18) for a rising ramp at the aggressor's input. Substituting (21)-(23) into equation (29), then solving the resulting equation, and using a normalized (with respect to V_{dd}) value for peak voltage, we obtain

$$V_p = \frac{\sqrt{m^2+m+1}}{m+1} \cdot \frac{2f_1}{T_W} \text{ (peak amplitude)} \quad (30)$$

$$T_0 = -\frac{f_2}{f_1} - \frac{m+2}{3\sqrt{m^2+m+1}} \cdot T_W \text{ (arrival time)} \quad (31)$$

$$T_1 = \frac{1}{\sqrt{m^2+m+1}} \cdot T_W \text{ (first transition time)} \quad (32)$$

$$T_2 = \frac{m}{\sqrt{m^2+m+1}} \cdot T_W \text{ (second transition time)} \quad (33)$$

where

$$T_W = \sqrt{\frac{36f_3}{f_1} - 18\left(\frac{f_2}{f_1}\right)^2} \quad (34)$$

The peak noise occurring time and pulse width can be obtained from the dependencies depicted in figure 2:

$$T_p = T_0 + T_1 = -\frac{f_2}{f_1} - \frac{m-1}{3\sqrt{m^2+m+1}} \cdot T_W \quad (35)$$

$$W_n = T_1 + T_2 = \frac{m+1}{\sqrt{m^2+m+1}} \cdot T_W \quad (36)$$

According to equation (24), we have $0 < m < \infty$. Hence, we obtain the lower and upper bounds for the corresponding parameters:

$$V_{pL} = \frac{\sqrt{3}}{2} \cdot \frac{2f_1}{T_W} \approx 0.87 \cdot \frac{2f_1}{T_W},\ V_{pU} = \frac{2f_1}{T_W} \quad (37)$$

$$T_{0L} = -\frac{f_2}{f_1} - \frac{2}{3} \cdot T_W,\ T_{0U} = -\frac{f_2}{f_1} - \frac{1}{3} \cdot T_W \quad (38)$$

$$T_{pL} = -\frac{f_2}{f_1} - \frac{1}{3} \cdot T_W,\ T_{pU} = -\frac{f_2}{f_1} + \frac{1}{3} \cdot T_W \quad (39)$$

$$W_{nL} = T_W,\ W_{nU} = \frac{2}{\sqrt{3}} \cdot T_W \approx 1.15 \cdot T_W \quad (40)$$

It is interesting to note that equations (37) and (40) give tight lower and upper bounds for peak amplitude and pulse width. For V_p, the difference is only around 13%, and for W_n, the difference is only around 15%.

Assuming $m = 1$, which indicates $T_1 = T_2$, we obtain a special case for equations (30) - (36):

$$V_p = \frac{\sqrt{3}f_1}{T_W} \text{ (peak amplitude)} \quad (41)$$

$$T_0 = -\frac{f_2}{f_1} - \frac{1}{\sqrt{3}} \cdot T_W \text{ (arrival time)} \quad (42)$$

$$T_1 = \frac{1}{\sqrt{3}} \cdot T_W \text{ (first transition time)} \quad (43)$$

$$T_2 = \frac{1}{\sqrt{3}} \cdot T_W \text{ (second transition time)} \quad (44)$$

$$T_p = -\frac{f_2}{f_1} \text{ (peak noise occurring time)} \quad (45)$$

$$W_n = \frac{2}{\sqrt{3}} \cdot T_W \text{ (pulse width)} \quad (46)$$

3.4 New noise metric II

Based on the mixed linear-exponential approximation, we set $V_o^{(j)}(s) = V_o^{(j)'}(s)$, and match the corresponding coefficients:

$$e_k^{(j)} = f_k^{(j)} \qquad (k = 1, 2, 3) \quad (47)$$

where $f_k^{(j)}$s are the moments of the noise output waveform, which can be computed by equations (11) to (14), and are simplified to equations (15) to (18) for a rising ramp at the aggressor's input. Substituting equations (26)-(28) into equation (47), and solving the above equation, we obtain the first transition time

$$T_1 = \frac{\frac{2m}{\lambda} + 1}{\sqrt{\frac{72m^4}{\lambda^4} + \frac{72m^3}{\lambda^3} + \frac{24m^2}{\lambda^2} + \frac{6m}{\lambda} + 1}} \cdot T_W \quad (48)$$

where T_W is given in equation (34). The peak noise amplitude is normalized with respect to power supply voltage V_{dd}, and we get

$$V_p = \frac{2f_1}{\frac{2m}{\lambda} + 1} \cdot \frac{1}{T_1} \text{ (peak amplitude)} \quad (49)$$

$$T_0 = -\left(\frac{f_2}{f_1}\right) - \left(\frac{\frac{6m^2}{\lambda^2} + \frac{6m}{\lambda} + 2}{\frac{6m}{\lambda} + 3} \cdot T_1\right) \text{ (arrival time)} \quad (50)$$

$$T_2 = mT_1,\ \tau_2 = \frac{m}{\lambda} \cdot T_1 \text{ (second transition time)} \quad (51)$$

$$T_p = -\left(\frac{f_2}{f_1}\right) - \left(\frac{\frac{6m^2}{\lambda^2} - 1}{\frac{6m}{\lambda} + 3} \cdot T_1\right) \text{ (peak occurring time)} \quad (52)$$

$$W_n = (m+1)T_1 \text{ (pulse width)} \quad (53)$$

In the above equations, m is unknown. We use an approximated value obtained from the piece-wise-linear model. First, set the initial value of T_1 to be the input transition time $T_1 = t_r$

Substituting the above value into equation (32), we get

$$m = \frac{\sqrt{4\left(\frac{T_W}{t_r}\right)^2 - 3} - 1}{2} \quad (54)$$

Now the parameters of the output crosstalk noise waveform can be computed using equations (48) to (53).

3.5 Discussion

Our modeling method can be applied to the flows summarized in figure 1. However, for the noise waveform (figure 1), we prefer to handle superposition in the time domain. This is because each aggressor is constrained by a timing window which determines the earliest and latest possible arrival times for its corresponding input [4]. Considering timing windows is essential in determining the worst-case crosstalk. Our modeling technique can also be applied to a mixture of rising and falling aggressor inputs.

4. MODEL VALIDATION

We have verified our new noise metric in 0.25μm technology for a variety of coupling circuits, including two-pin nets and RC trees, shown in figure 4. We compute the parameters of the noise waveform for over 40000 cases, with different coupling locations, driver strengths, coupling lengths, etc. In addition to the coupling circuits with parameters of normal ranges, we have run experiments for some extreme corner cases, including some in which the victim and aggressor driver sizes differ drastically, the coupling location is far away or very close to the victim driver, far away or very close to the victim receiver, etc. And the coupling length ranges from 0.1*mm* to 2.0*mm*. Thus, the results we report here show a larger error percentage than the results reported in the original papers [7][13][17]. Table 1 gives results for two-pin net coupling circuits with far-end coupling direction when the victim's receiver is closer to the aggressor's receiver than to the aggressor's driver. Different analytical methods are compared with Hspice simulation. The maximum and average error percentages are shown for the computation of crosstalk noise metrics, including peak amplitude V_p, pulse width W_n, peak noise occurring time T_p, the first transition time T_1, and the second transition time T_2. The average error percentage is computed over the absolute error percentage values. For the peak noise amplitude, we show both the

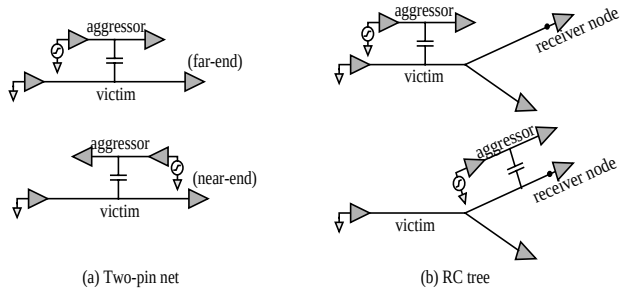

Figure 4. Coupling circuit structure for experiments

maximum positive error percentage and the maximum negative error percentage. Table 2 gives results for two-pin net coupling circuits with near-end coupling direction. Usually near-end coupling causes larger crosstalk noise. Table 3 presents the results for distributed RC trees. When the maximum negative error percentage is within the range from -5% to 0, we still consider this metric to be conservative, so it can be used as an upper bound. The entries "N/A"s in the tables indicate that the corresponding method does not capture the parameter of this row, whereas our new metrics are capable of a complete characterization of the noise waveform.

The results presented in table 1 identify three metrics as the upper bounds of peak noise for a far-end coupling circuit: [7], [13] and our new metric II. Our new metric provides the tightest upper bound. The results presented in table 2 identify only one metric as the upper bound of peak noise estimation for a near-end coupling circuit. This is our new metric II. We can see that the simple metrics given by [7] and [13] fail to capture the difference between far-end and near-end coupling. Those methods do not provide upper bounds for the near-end coupling noise because the near-end peak noise is usually larger than the far-end noise[13].

An interesting fact about our second new noise metric is that the results can be affected by the value of λ. When we use the default value given in equation (7), we can obtain an absolute upper bound for the peak noise amplitude. It has a relatively larger error percentage, but is still tighter than Vittal's upper bound. Our second new metric is much better than the first one. It provides a better upper bound (for peak noise amplitude) than all the existing metrics. The major problem with the two-pole model and the improved one pole model proposed in [17] is that their metric is not conservative, and the estimated peak noise could be much smaller than the actual peak noise. Besides, the two-pole model suffers from instability and may not offer a solution for some circuits.

Table 1: Error percentage for two-pin nets, far-end coupling

Crosstalk noise metrics		Yu's improved 1 pole model [17]	Yu's 2 pole model [17]	Devgan [7]	Vittal [13]	new I	new II (λ=2.7465)
V_p	Max. (%)	-26 ~ 38	-28 ~ 0	-3 ~ 1330	-3 ~ 85	-39 ~ 49	0 ~ 42
	Ave. (%)	15	19	91	20	21	16
W_n	Max. (%)	N/A	N/A	N/A	120	71	85
	Ave. (%)				64.7	13	12
T_p	Max. (%)	N/A	85	N/A	N/A	72	31
	Ave. (%)		21			27	13
T_1	Max. (%)	N/A	N/A	N/A	N/A	81	63
	Ave. (%)					12	11
T_2	Max. (%)	N/A	N/A	N/A	N/A	101	73
	Ave. (%)					21	35

Table 2: Error percentage for two-pin nets, near-end coupling

Crosstalk noise metrics		Yu's improved 1 pole model [17]	Yu's 2 pole model [17]	Devgan [7]	Vittal [13]	new I	new II (λ=2.7465)
V_p	Max. (%)	-41 ~ 35	-38 ~ 0	-9 ~ 1309	-20 ~ 85	-45 ~ 36	0 ~ 51
	Ave. (%)	18	23	83	18	24	20
W_n	Max. (%)	N/A	N/A	N/A	126	83	84
	Ave. (%)				65	14	14
T_p	Max. (%)	N/A	99	N/A	N/A	78	39
	Ave. (%)		24			31	14
T_1	Max. (%)	N/A	N/A	N/A	N/A	81	82
	Ave. (%)					12	11
T_2	Max. (%)	N/A	N/A	N/A	N/A	99	71
	Ave. (%)					22	36

Table 3: Error percentage for tree structures, far-end coupling

Crosstalk noise metrics		Yu's improved 1 pole model [17]	Yu's 2 pole model [17]	Devgan [7]	Vittal [13]	new I	new II (λ=2.7465)
V_p	Max. (%)	-22 ~ 37	-26 ~ 0	-3 ~1320	0 ~ 84	-33 ~ 36	0 ~ 41
	Ave. (%)	14	19	92	21	21	17
W_n	Max. (%)	N/A	N/A	N/A	120	87	73
	Ave. (%)				64	13	14
T_p	Max. (%)	N/A	38	N/A	N/A	37	33
	Ave. (%)		21			24	14
T_1	Max. (%)	N/A	N/A	N/A	N/A	63	46
	Ave. (%)					14	12
T_2	Max. (%)	N/A	N/A	N/A	N/A	85	91
	Ave. (%)					22	25

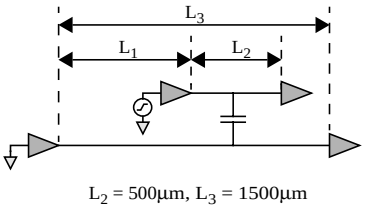

(a) The coupling circuit

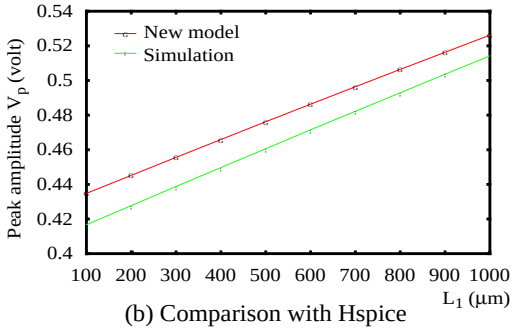

(b) Comparison with Hspice

Figure 5. Coupling location affects crosstalk noise

Figure 5 shows the effect of coupling location on the peak amplitude of the crosstalk noise. In this group of experiments, we set L_2 = *0.5mm*, L_3 = *1.5mm*, and change L_1 from *0.1mm* to *1.0mm*. The closer the aggressor to the victim receiver node, the larger the peak noise on this node. A nearly linear increase of the peak noise amplitude with the change of coupling location can be observed. Though the lumped π-model will report the same peak noise voltage for every coupling location described in figure 5, our model captures the above trend very well.

In the presence of multiple aggressors, the method described in [4] can be applied to compute the combined maximum (worst-case) peak noise amplitude. However, no methods exist which are capable of estimating the worst-case pulse-width, or the worst-case noise transition time for the combined noise waveform. We leave this part for our future research.

5. CONCLUSIONS

In deep submicron designs, a signal transition on interconnects running in close proximity can lead to unexpected spikes on normally static signals, or change the delays of switching signals, consequently causing performance degradation or functional failure. These are the crosstalk effects. It is essential to develop metrics to estimate them quickly and accurately.

We have proposed a classification of the existing methods, and pointed out their weaknesses, such as insufficient characterization of the noise phenomenon other than the peak amplitude, ignoring the rise and fall transition times, high complexity, or low accuracy. We proposed a new backend noise analysis methodology which thoroughly captures the features of crosstalk noise waveform, maintains a balance between complexity and accuracy, and provides a better upper bound for peak noise amplitude estimation in all types of coupling scenarios. Our approach provides closed-form crosstalk noise metrics which are applicable to any distributed coupled RC tree networks. It is fast, conservative, and yet achieves acceptable accuracy. It can be safely included in the inner loop and early stages of design flow.

ACKNOWLEDGEMENT

This work was supported in part by the NSF grant # CCR-0098069 and in part by the California MICRO program through Mindspeed and Synopsys.

REFERENCES

[1] E. Acar, A. Odabasioglu, M. Celik, and L. T. Pileggi, “S2P: a stable 2-pole RC delay and coupling noise metric,” in *Proc. Ninth Great Lakes Symposium on VLSI*, March 1999, pp.60-63.

[2] L. H. Chen, M. Marek-Sadowska, R. Divecha, and P. Singh, “Capturing Input Switching Dependency In Crosstalk Noise Modeling,” in *Proc. Int. ASIC/SOC Conf.*, 2000, September 2000, p.330-334.

[3] C. -W. Chang, C. -K. Cheng, P. Suaris, and M. Marek-Sadowska, "Fast Post-placement Rewiring Using Easily Detectable Functional Symmetries," *Design Automation Conf. 2000*.

[4] L. H. Chen and M. Marek-Sadowska, “Aggressor alignment for worst-case crosstalk noise,” IEEE Tran. Computer-Aided Design, vol. 20, no. 5, pp. 612-621., May 2001.

[5] W. Chen, S. K. Gupta, and M. A. Breuer, “Analytic models for crosstalk delay and pulse analysis under non-ideal inputs,” in *Proc. IEEE Int. Test Conf.*, 1997, pp.809-818.

[6] J. Cong, D. Z. Pan, and P. V. Srinivas, “Improved crosstalk modeling for noise constrained interconnect optimization,” in *Proc. ACM/IEEE International Workshop on Timing Issues in the Specification and Synthesis of Digital Systems*, Dec. 2000, pp. 14-20.

[7] A. Devgan, “Efficient coupled noise estimation for on-chip interconnects,” in *Proc. ICCAD*, Nov. 1997, pp.147-153.

[8] P. Feldmann and R. W. Freund, “Efficient linear circuit analysis by Pade approximation via the Lanczos process,” IEEE Tran. Computer-Aided Design of Intergrated Circuits and Systems, vol.14, no. 5, pp.639-649, May 1995.

[9] A. B. Kahng, S. Muddu, and D. Vidhani, “Noise and delay uncertainty studies for coupled RC interconnects,” in *Proc. IEEE International ASIC/SOC Conference*, Sep. 1999, pp.3-8.

[10] M. Kuhlmann and S. S. Sapatnekar, Exact and efficient crosstalk estimation, *IEEE Transactions on Computer-Aided Design of Integrated Circuits and Systems*, vol.20, no.7, pp.858-66, July 2001.

[11] J. Millman and A. Grabel, *Microelectronics*, 2nd ed. New York: McGraw Hill, 1987, pp.483-484.

[12] L. T. Pillage and R. A. Rohrer, “Asympototic waveform evaluation for timing analysis,” *IEEE Trans. Computer-Aided Design*, vol.9, pp.352-366, Apr.1990.

[13] A. Vittal, L. H. Chen, M. Marek-Sadowska, K.-P. Wang, and S. Yang, “Crosstalk in VLSI interconnections,” *IEEE Transactions on Computer-Aided Design of Integrated Circuits and Systems*, vol.18, (no.12). p.1817-24, Dec. 1999.

[14] A. Vittal and M. Marek-Sadowska, “Crosstalk reduction for VLSI,” *IEEE Trans. Computer-Aided Design*, vol.16, pp.290-298, Mar.1997.

[15] T. Xiao and M. Marek-Sadowska, “Efficient delay calculation in presence of crosstalk,” in *Proceedings IEEE 2000 First International Symposium on Quality Electronic Design*, March 2000, pp.491-497.

[16] Q. Yu and E. Kuh, “Moment computation of lumped and distributed coupled RC trees with application to delay and crosstalk estimation,” *Proc. of the IEEE*, vol. 89, no.5, pp. 772-788, May 2001.

[17] Q. Yu and E. Kuh, “New efficient and accurate matching based model for crosstalk estimation in coupled RC trees,” in *Proc. International Symposium on Quality Electronic Design*, March 2001, pp.151-157.